

ARTICLE

Open Access



Ellagic acid exerts anti-fibrotic effects on hypertrophic scar fibroblasts via inhibition of TGF- β 1/Smad2/3 pathway

Xianjun Liu^{1,2†}, Xinxin Gao^{3,4†}, Hao Li^{1,2}, Zhandong Li^{1,2}, Xiaoe Wang¹, Li Zhang¹, Bo Wang⁵, Xinxin Chen^{3,4}, Xianglong Meng^{3,4*}  and Jiaao Yu^{3,4*}

Abstract

Hypertrophic scar (HS) is a kind of serious pathological scar with no currently effective treatment. HS fibroblasts (HSFs) are the main effector cells for HS formation. Ellagic acid (EA) exerts regulatory effects in some diseases, but its role in HS remains unclear. This study aimed to evaluate the effect of EA on the fibrotic phenotypes of HSFs and to further investigate the downstream signaling mechanism. The cell counting kit-8 (CCK-8) assay was used to perform cytotoxicity and proliferation assays. HSFs migration was assessed using wound healing and transwell assays. HSFs contraction was measured by a collagen lattice contraction assay and detection of α -smooth muscle actin (α -SMA) expression. The levels of mRNA and protein were determined by qPCR and western blotting, respectively. The results showed that EA inhibited the proliferation, migration, and contraction of HSFs and collagen expression in HSFs in a dose-dependent manner. Furthermore, EA not only suppressed the Smad2/3 pathway but also reversed TGF- β 1-induced activation of the Smad2/3 pathway and up-regulation of the fibrotic cellular phenotypes in HSFs. These findings demonstrate that EA exerts anti-fibrotic effects on HSFs by blocking the TGF- β 1/Smad2/3 pathway, which indicates that EA is a potential therapeutic candidate for treatment of HS.

Keywords: Collagen, Contraction, Ellagic acid, Hypertrophic scar fibroblasts, Migration, Proliferation, Smad pathway, TGF- β 1

Introduction

Hypertrophic scar (HS) is a severe skin fibrotic disease that often occurs after burn injury. HS is generally raised, red, itchy, or painful, and can even lead to movement dysfunction. These adverse symptoms result in not only physical but also psychological injury to the patients [1]. Statistics show that up to 70% of burn patients suffer from HS [2]. In recent years, a few treatments have been developed; however, there is currently no effective therapy for HS. Previous studies have demonstrated that

the pathological mechanism of HS formation is mainly identified by aberrant deposition of extracellular matrix (ECM), especially collagen I and III, and overactive hypertrophic scar fibroblasts (HSFs) are the effector cells contributing to the progression of HS [3]. It is meaningful to explore an approach that could effectively attenuate the fibrotic cellular phenotypes of HSFs, including proliferation, migration, contraction, and collagen expression.

Ellagic acid (EA) (molecular formula $C_{14}H_6O_8$, Fig. 1A) is a natural plant polyphenolic compound that is abundant in various fruits and nuts. Previous studies have mostly focused on the antioxidant, antihepatotoxic, and antitumor effects of EA [4–6]. Additionally, a few studies have indicated that EA exerts anti-fibrotic effects in liver, pancreatic, and cardiac fibrosis [7–9]. However, the effect of EA on HS formation remains unclear.

*Correspondence: mengxldyy@jlu.edu.cn; yuja@jlu.edu.cn

[†]Xianjun Liu and Xinxin Gao contributed equally to this work

³ Department of Burns Surgery, The First Hospital of Jilin University, No. 1409 Ximinzhong Street, Changchun 130000, China

Full list of author information is available at the end of the article

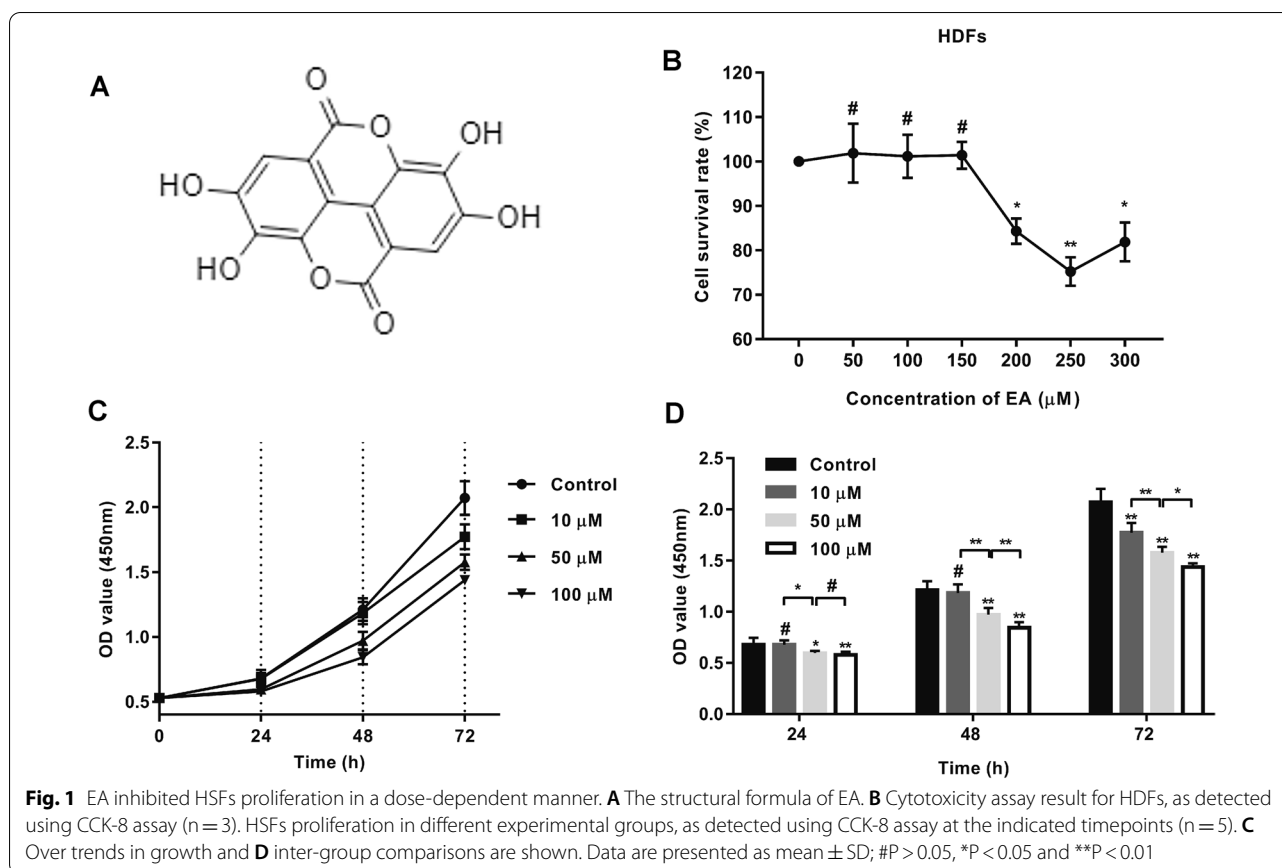


Fig. 1 EA inhibited HSFs proliferation in a dose-dependent manner. **A** The structural formula of EA. **B** Cytotoxicity assay result for HDFs, as detected using CCK-8 assay ($n = 3$). HSFs proliferation in different experimental groups, as detected using CCK-8 assay at the indicated timepoints ($n = 5$). **C** Over trends in growth and **D** inter-group comparisons are shown. Data are presented as mean \pm SD; # $P > 0.05$, * $P < 0.05$ and ** $P < 0.01$

The Smad2/3 signaling pathway is a canonical fibrosis-associated signal transduction pathway, activation of which regulates a spectrum of pathological cellular behaviors of HSFs [3]. TGF- β 1, a well-known pro-fibrotic growth factor, is a significant upstream stimulator of the Smad2/3 pathway. Previous studies have found that TGF- β 1 promotes the proliferation, migration, and contraction of HSFs and collagen synthesis in HSFs by activating the Smad2/3 pathway [10]. Proper regulation of the TGF- β 1/Smad2/3 pathway in HSFs is considered a promising strategy for hindering HS formation.

In this study, we evaluated the effects of EA on the proliferation, migration, and contraction of HSFs and collagen expression in HSFs. Importantly, we further investigated the association between the TGF- β 1/Smad2/3 pathway and EA-induced regulation of HSFs.

Materials and methods

Antibodies and drugs

The primary antibodies used for western blotting in this study were as follows: anti- α -smooth muscle actin (α -SMA) (1:1000; cat. no. ab32575; Abcam, Cambridge, UK), anti-collagen I (1:1000; cat. no. AF7001; Affinity, OH, USA), anti-collagen III (1:1000; cat. no. AF0136;

Affinity), anti-Smad2 (1:5000; cat. no. ab40855; Abcam), anti-Smad2 (phospho S255) (1:5000; cat. no. ab188334; Abcam), anti-Smad3 (1:5000; cat. no. ab40854; Abcam), anti-Smad3 (phospho S423 + S425) (1:2000; cat. no. ab52903; Abcam), and anti-GAPDH (1:5000, cat. no. 10494-1-AP; Proteintech, IL, USA). Secondary antibodies (1:5000; goat anti-mouse cat. no. SA00001-1; goat anti-rabbit cat. no. SA00001-2; Proteintech) were used for western blotting. EA (cat. no. B21073; Yuanye Biotech, Shanghai, China) was dissolved in 1 M NaOH. The final concentration of NaOH was $\leq 0.1\%$ (v/v) and did not contribute to toxicity. TGF- β 1 (cat. no. bs-2266P; Bioss, Beijing, China) was diluted with sterile double-distilled water.

Cells isolation and culture

Normal human dermal fibroblasts (HDFs) (cat. no. #2320) were purchased from Sciencell, and three cell lines were obtained for subsequent cytotoxicity assay by parallel culture. HSFs were primarily cultured from the scar tissues of five patients (3 men and 2 women; aged 10–50 years) who suffered HS and had a cicatrixectomy in the Department of Burns Surgery of the First Hospital of Jilin University between January and April 2018.

Protocols were approved by the Ethics Committee of the First Hospital of Jilin University (no. 2017-088) and were conducted according to the principles expressed in the Declaration of Helsinki. Written informed consent was obtained from all donors before surgery. Briefly, the epidermis and subcutaneous adipose tissue of HS tissue masses were shaped. Next, the tissues were cut into approximately 1 mm³ sections under sterile conditions. After washing, sections were placed in a cell culture dish and incubated in Dulbecco's modified Eagle's medium (DMEM) containing 10% fetal bovine serum (FBS) and double antibiotics (penicillin, 100 U/mL; streptomycin, 0.1 mg/mL) at 37 °C with 5% CO₂. All cell culture reagents were supplied by Gibco (Thermo Fisher Scientific, MA, USA). When fibroblasts reached approximately 90% confluence, they were trypsinized and passaged. Cells from passages 2–4 were used in the subsequent experiments.

Cytotoxicity and proliferation assays

A cell counting kit 8 (CCK-8) assay was used for cytotoxicity and proliferation assays. Viable HDFs or HSFs counts were indirectly detected by measuring the optical density (OD) values. Cytotoxicity assay was performed as described below. Briefly, HDFs were seeded at 2×10^4 cells per well in a 96-well culture plate, with three replicates per sample, excluding the use of external rows and columns, to avoid edge effects. After complete cell attachment, HDFs were processed according to the experimental requirements. After treatment for 48 h, 10 μ L of CCK-8 (APEX-BIO, Houston, USA) solution was added to each well. After incubation for 2 h at 37 °C, the absorbance was measured at 450 nm wavelength using a microplate reader (Thermo Fisher Scientific, MA, USA). The cytotoxicity assay results were expressed as cell survival rates. Cell survival rate (%) = (OD value of treated group - OD value of blank) / (OD value of control group - OD value of blank) \times 100. As for the proliferation assay, HSFs were seeded at 5×10^3 cells per well in a 96-well culture plate, and the OD values were tested at time points 0, 24, 48, and 72 h after treatment. In addition to these, the method of OD value detection was the same as the cytotoxicity assay. The proliferation assay results were expressed as OD values.

Wound healing assay

A wound healing assay was used to assess the migration of HSFs. In brief, HSFs were cultured in a 6-well culture plate at a density of 1×10^4 cells/cm² with DMEM containing 10% FBS until the cell confluence reached 100%. A scratch wound was made in the middle of each well using a 1-mL pipette tip. After washing with PBS, the culture medium was changed to serum-free DMEM, with

EA or TGF- β 1 according to experimental requirements. At the time points 0, 24, and 48 h after scratching, images were acquired at three random fields of view using an inverted microscope (magnification 40 \times ; Olympus Corporation, Tokyo, Japan). Wound area was measured using ImageJ software (version 1.51w). Migration ability of HSFs was evaluated using the data shown as migration rate (%) = (initial wound area - wound area at 24 or 48 h) / initial wound area \times 100.

Transwell assay

A transwell assay was used to assess the migration of HSFs. Briefly, 2×10^5 HSFs were seeded in the upper chambers of transwell plates (6-well, 8 μ m; Millicell, MA, USA) incubated in serum-free DMEM, and the lower chambers were supplied with DMEM containing 10% FBS, with EA or TGF- β 1 according to experimental requirements. After 24 h, non-migrated HSFs on the upper face of the polycarbonate membrane were removed with a cotton swab, and migrated HSFs were fixed with methanol and stained with Giemsa dye solution (cat. no. R20649; Yuanye Biotech, Shanghai, China). Images of each well were captured at three random fields of view using an OLYMPUS inverted microscope. The cells were counted using ImageJ software.

Collagen lattice contraction assay

A collagen lattice contraction assay was used to assess the contraction ability of HSFs. HSFs were mixed with rat tail tendon collagen (cat. no. C8062; Solarbio, Beijing, China). The final collagen concentration of the mixture was 1 mg/mL, with a cell density of 2.5×10^5 cells/mL. The mixture was added to a 24-well cell culture plate (200 μ L/well) and incubated at 37 °C for 1 h. After coagulation, 500 μ L serum-free DMEM, with EA or TGF- β 1 according to experimental requirements, was added onto the gel. A picture of each sample was captured at 48 h. The area of the gels calculated using ImageJ software. The contraction rate was presented as a measure of HSFs contraction: contraction rate (%) = (well area - gel area) / well area \times 100.

Real-time quantitative PCR (qPCR)

RNA was isolated, and qPCR was carried out. Briefly, total RNA was isolated from the samples using TRIzol[®] reagent (Invitrogen, USA). cDNA was synthesized using the TransScript All-in-One First-Strand cDNA Synthesis SuperMix (TransGen Biotech, Beijing, China). FastStart Universal SYBR Green Master (ROX) (Roche Diagnostics, Mannheim, Germany) was used for qPCR with a Stratagene Mx3005P instrument (Agilent Technologies, USA). The reaction conditions were as follows: initial denaturation at 95 °C for 10 min; 40

cycles of denaturation at 95 °C for 30 s and annealing at 60 °C for 1 min; dissociation at 95 °C for 1 min, annealing at 55 °C for 30 s, and final extension at 95 °C for 30 s. The primers used in qPCR are listed in Table 1. The expression levels of target genes were normalized to that of GAPDH, and the $2^{-\Delta\Delta C_t}$ method was used to calculate the relative mRNA levels [11]. Each sample was run in triplicate.

Western blotting

Harvested fibroblasts were processed with RIPA lysis buffer (CST, USA) supplemented with phenylmethylsulphonyl fluoride (Thermo Fisher Scientific, MA, USA), protease inhibitor cocktail (TransGen Biotech, Beijing, China), and phosphatase inhibitor cocktail (TransGen Biotech). Protein concentration was measured using a bicinchoninic acid (BCA) protein assay kit (Beyotime Institute of Biotechnology, Nantong, China). Samples were separated using SDS-PAGE gels, and subsequently electro-transferred to PVDF membranes (Millipore, MA, USA) for immunoblotting analysis. After blocking with 5% bovine serum albumin (Sigma-Aldrich, MO, USA) in TBST (0.5% Tween-20) for 1 h at room temperature, the PVDF membranes were incubated with primary antibodies at 4 °C overnight. Following incubation with the appropriate horseradish peroxidase-conjugated secondary antibodies for 1 h at room temperature, proteins were detected with the EasySee western blotting kit (TransGen Biotech) using a myECL™ imager (Thermo Fisher Scientific), and the band intensities were quantified by calculation of gray values using ImageJ software. Data were collected from three independent experiments.

Statistical analysis

The quantified data are presented as the mean ± standard deviation (SD). The differences between the two groups were analyzed by Student's t-test using the

GraphPad Prism (version 7.00) statistical package. A value of $P < 0.05$ indicated a statistically significant difference.

Results and discussion

EA inhibited HSFs proliferation in a dose-dependent manner

First, we performed cytotoxicity assay for EA to HDFs by a CCK-8 assay. As shown in Fig. 1B, there was no significant difference in cell survival rate between each EA-treated group (concentration $\leq 150 \mu\text{M}$) and the control group. This result suggested a concentration range, at which EA is harmless to normal HDFs. Then, to evaluate the effect of EA on HSFs proliferation, a CCK-8 assay was performed. As shown in Fig. 1C and D, HSFs proliferation in the EA-treated groups was attenuated as compared with that of the control group. There was no significant difference in cell viability between the 10 μM group and the control group at 24 and 48 h. The data demonstrated a significant decrease in HSFs proliferation in the 10 μM group as compared with that of the control group at 72 h; HSFs proliferation in the 50 and 100 μM groups was significantly lower than that of the control group at all time points. Additionally, HSFs proliferation in the 50 and 100 μM groups was significantly lower than that of the 10 μM group at all time points. HSFs proliferation in the 100 μM group was significantly lower than that of the 50 μM group at all time points except for 24 h. All these data indicate that EA inhibited HSFs proliferation in a dose-dependent manner.

EA inhibited HSFs migration in a dose-dependent manner

The effect of EA on HSFs migration was assessed using wound healing and transwell assays. As shown in Fig. 2A and 2B, at 24 and 48 h after scratching, the migration rate of HSFs significantly decreased with increasing EA dose. In addition, the results of the transwell assay (Fig. 2C and 2D) showed that the migrated HSFs were significantly reduced with increasing EA dose, consistent with the results of wound healing assay. These data demonstrate that EA inhibited HSFs migration in a dose-dependent manner.

EA inhibited HSFs contraction in a dose-dependent manner

To evaluate the effect of EA on HSFs contraction, a collagen lattice contraction assay was performed, and the expression of α -SMA, which is correlated with the contractive ability of HSFs, was detected using qPCR and western blotting. As shown in Fig. 3A and B, with increasing EA dose, the contraction rate significantly decreased. As for the detection of α -SMA, encoded by *ACTA2* gene, the data of qPCR showed that the mRNA level of *ACTA2*

Table 1 Sequences of primers for qPCR

	Forward (5' → 3')	Reverse (5' → 3')
<i>ACTA2</i>	GACAATGGCTCTGGGCTC TGTA	TGTGCTTCGTACCCACGTA
<i>COL1A1</i>	ACCAGTCTCCATGTTGCA GAAGA	CGTGACCTCAAGATGTGCCACT
<i>COL1A2</i>	GAGGGCAACAGCAGGTTC ACTTA	TCAGCACCACCGATGTCCA
<i>COL3A1</i>	CCACGGAAACACTGGTGGAC	GCCAGCTGCACATCAAGGAC
<i>GAPDH</i>	GCACCGTCAAGCTGAGAAC	TGGTGAAGACGCCAGTGGAA

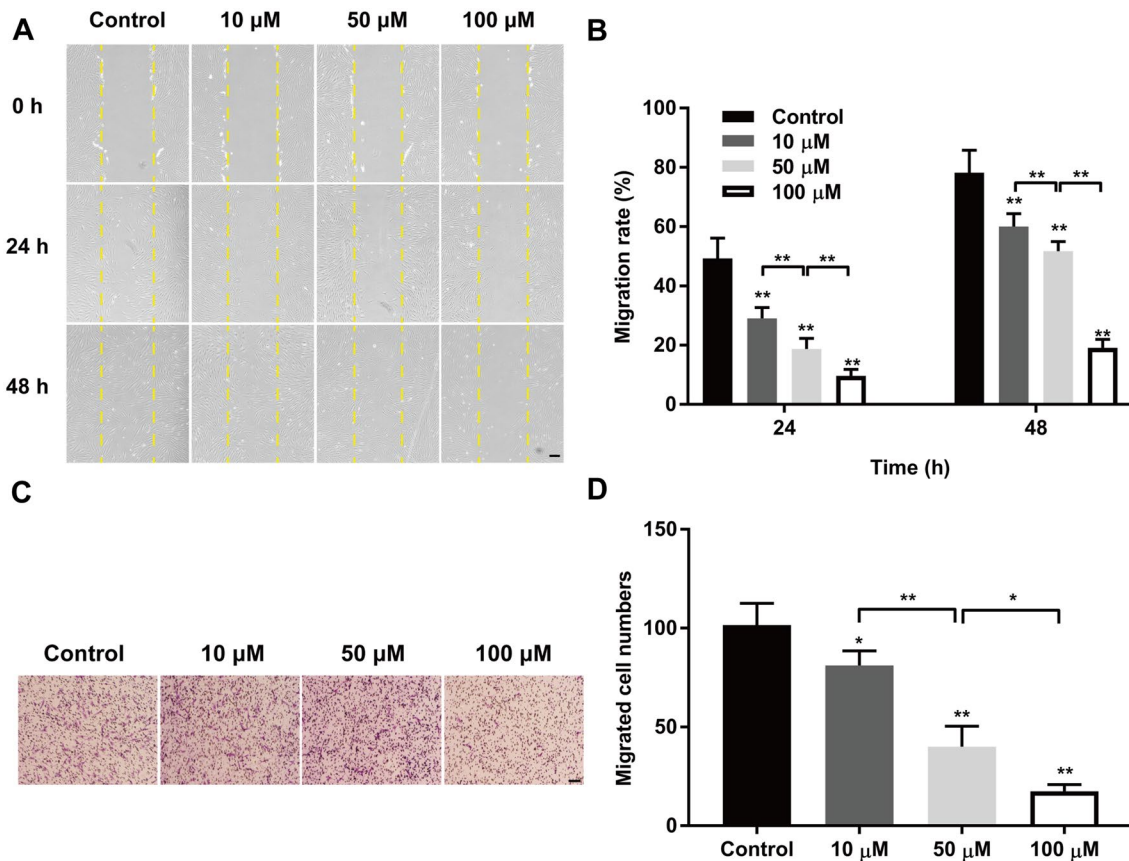


Fig. 2 EA inhibited HSFs migration in a dose-dependent manner. HSFs proliferation in different experimental groups, as detected using a wound healing assay at the indicated timepoints ($n = 5$). **A** Representative pictures (scale bar = 200 μm), and **B** quantitative analysis of migration rate (%) and inter-group comparison are shown. HSFs proliferation in different experimental groups, as detected using a transwell assay after 24 h of treatment ($n = 5$). **C** Representative pictures (scale bar = 100 μm) and **D** quantitative analysis of migrated cell numbers are shown. Data are presented as mean \pm SD; * $P < 0.05$ and ** $P < 0.01$

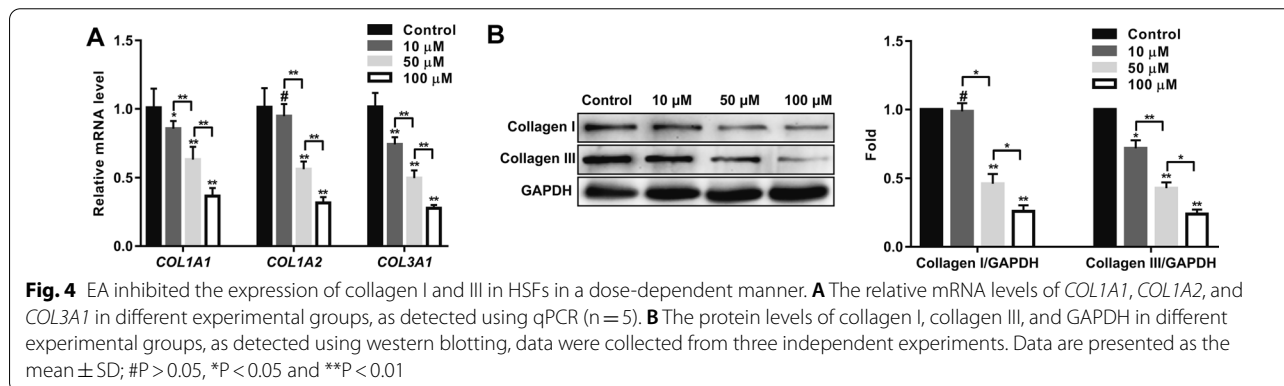
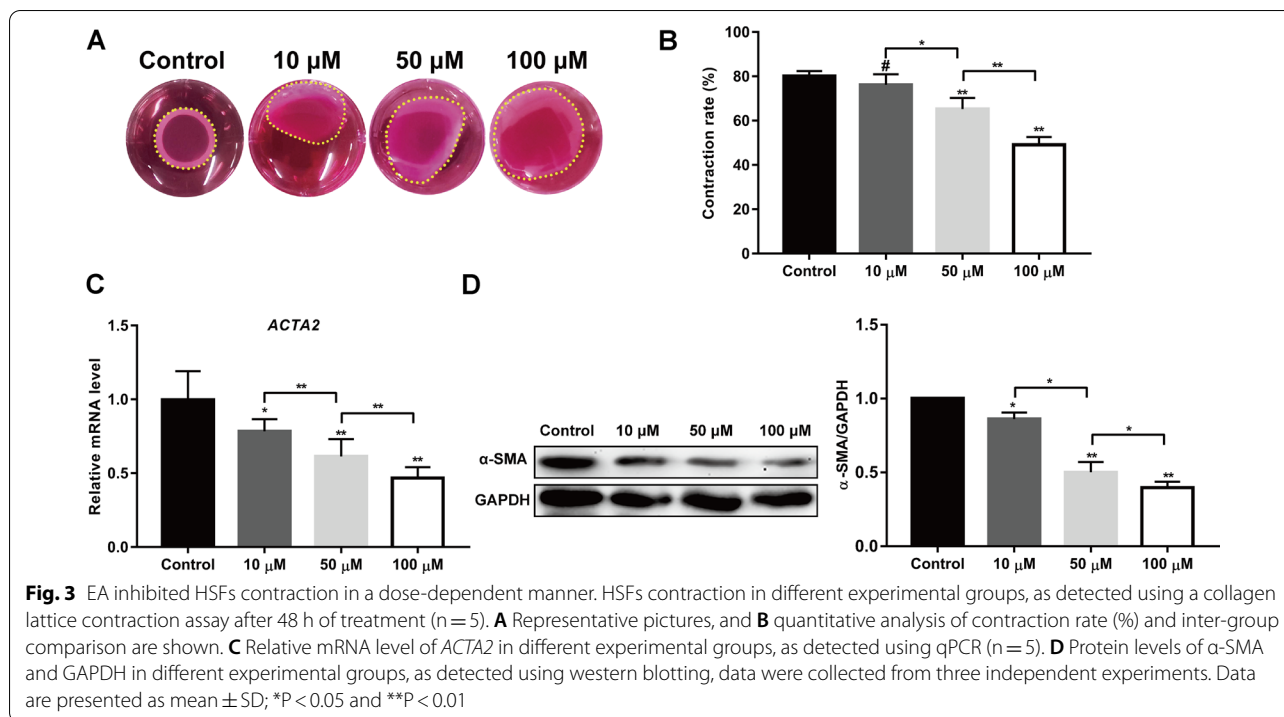
decreased with an increase in EA dose (Fig. 3C). Western blotting showed that the change in α -SMA protein level was in line with that of its mRNA level. All these measures indicated that EA inhibited HSFs contraction in a dose-dependent manner.

EA inhibited the expression of collagen I and III in HSFs in a dose-dependent manner

To evaluate the effect of EA on collagen synthesis in HSFs, qPCR and western blotting were used to detect the mRNA and protein levels of collagen I and III, respectively. As shown in Fig. 4A, the mRNA levels of *COL1A1*, *COL1A2*, and *COL3A1* were significantly reduced with increasing EA dose, in addition to *COL1A2* expression in the 10 μM group. The change in protein levels of collagen I and III was consistent with the change in mRNA levels (Fig. 4B). These results demonstrate that EA inhibited the expression of collagen I and III in HSFs in a dose-dependent manner.

EA inhibited TGF- β 1/Smad2/3 signaling pathway in HSFs

Based on the above findings, we assessed the effect of EA on HS-associated signaling pathway in HSFs. The protein levels of total (t)-Smad2, p-Smad2, t-Smad3, and p-Smad3 were detected using western blotting, and the ratios of p-Smad2/t-Smad2 and p-Smad3/t-Smad3 were calculated to evaluate the Smad2/3 pathway. As shown in Fig. 5A and B, the ratios of p-Smad2/t-Smad2 and p-Smad3/t-Smad3 significantly decreased in the EA-treated group (100 μM), and significantly increased in the TGF- β 1-treated group (10 ng/mL) as compared with those in the control group. Furthermore, EA treatment significantly reversed TGF- β 1-induced up-regulated phosphorylation of Smad2 and 3. These data indicated that EA inhibited the TGF- β 1/Smad2/3 signaling pathway in HSFs.



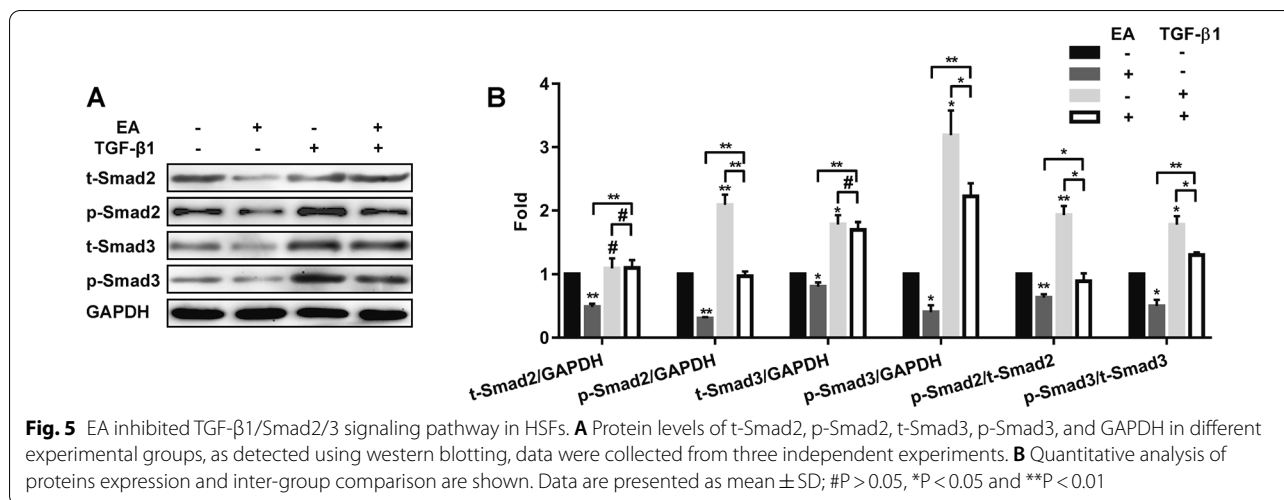
EA inhibited TGF- β 1-induced up-regulation of HSFs proliferation, migration, and contraction, and collagen synthesis in HSFs

To further investigate the association between EA-induced inhibition of fibrotic phenotypes and TGF- β 1/Smad2/3 signaling pathway in HSFs, we measured the effect of EA (100 μ M) on TGF- β 1-induced up-regulation of HSFs proliferation, migration, and contraction, and collagen synthesis in HSFs. The results showed that EA significantly reversed TGF- β 1-induced up-regulation of proliferation as assessed by CCK-8 assay (Fig. 6A), migration as assessed by wound healing assay (Fig. 6B) and

transwell assay (Fig. 6C), contraction as assessed by collagen lattice contraction assay (Fig. 6D) and α -SMA detection (Fig. 6E and F), and collagen synthesis as assessed by collagen I and III detection (Fig. 6E and F). These results demonstrate that EA exerted inhibitory effects on TGF- β 1-induced fibrotic phenotypes of HSFs.

Discussion

HS, which often occurs after burn injury, is gradually becoming a challenge for clinical workers [1]. Although a few therapies, such as laser therapy, compression garments, and topical drug application, have



been developed, there is not yet a satisfactory treatment for HS [12]. In recent years, pre-clinical studies have indicated that some natural plant extracts exhibit anti-fibrotic properties in vitro and/or in vivo [13–15]. Natural extracts are often well-tolerated. Our work, for the first time, has demonstrated that EA attenuated multiple fibrotic phenotypes of HSFs in vitro.

The over-proliferation of HSFs is considered to be associated with HS formation. In studies on the role of EA in fibrotic diseases, to date, EA was reported to exert a hindering effect on the growth of rat PDGF-treated pancreatic stellate cells [16] and rat cardiac fibroblasts [9]. Similarly, our work showed that EA significantly inhibited HSFs proliferation (Fig. 1). Moreover, various studies focusing on the role of EA in multiple cancer types have also reported its inhibitory effect on cell proliferation [6].

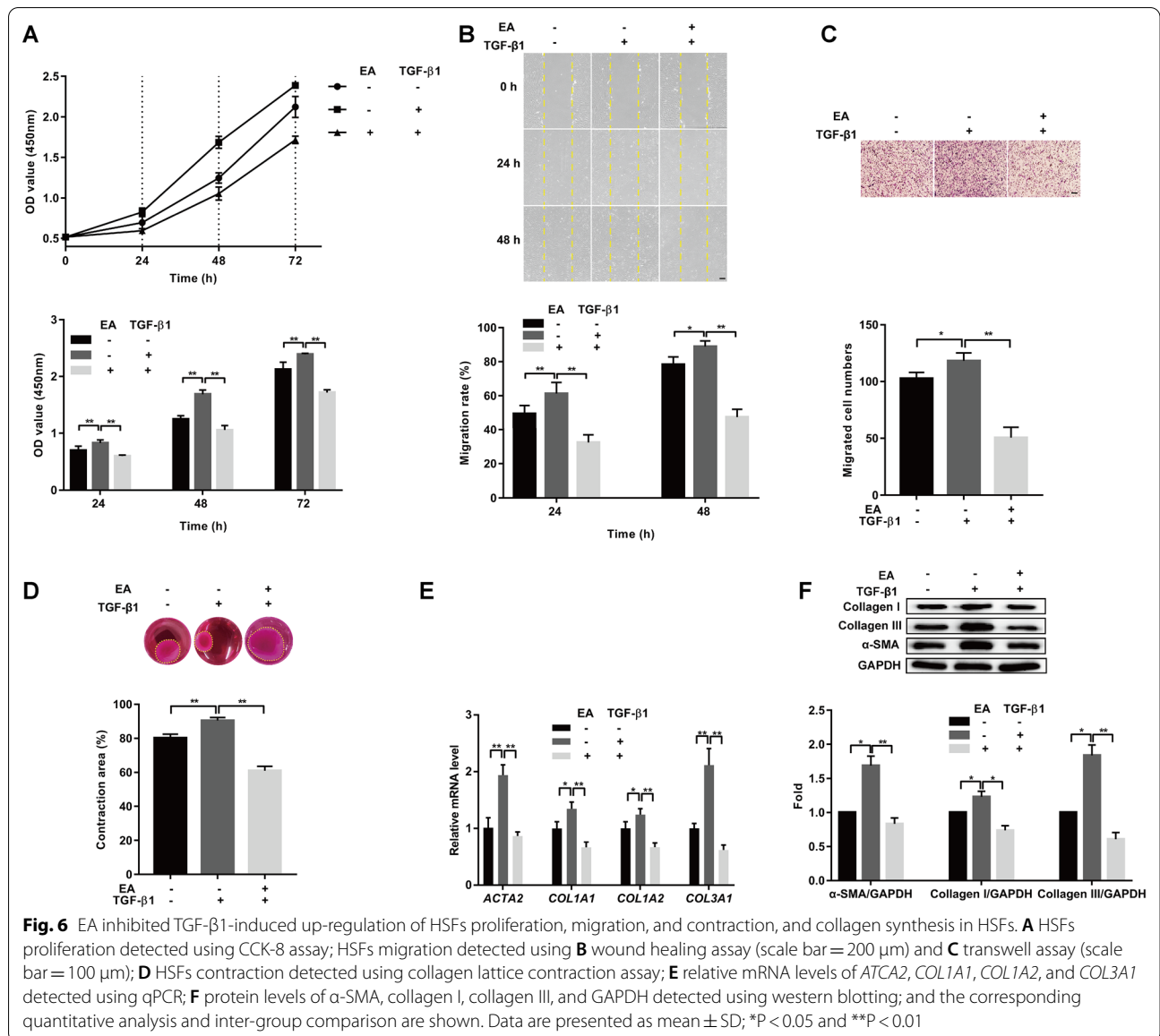
Studies on enhanced migration, a pathological cellular behavior of HSFs, are gradually increasing. In addition to the inhibitory action of EA on the migration of a few cancer cell lines [6], Masamune et al. found that EA attenuated PDGF-induced migration of pancreatic stellate cells [16], and Lin et al. found similar inhibitory effect of EA on rat cardiac fibroblasts [9]. Consistent with these studies, our work found that EA suppressed HSFs migration (Fig. 2).

The contraction of human dermal fibroblasts plays an important role in wound healing, but excessive contraction of HSFs contributes significantly to the inelasticity and contracture of HS [17]. Some previous studies have reported that EA could reduce the ventricular myocytes of mice and rats in vitro [18, 19]. Similarly, our results indicated that EA inhibited HSFs contraction (Fig. 3).

These findings illustrate the similar effect of EA on the same phenotypes of different diseases cells.

Collagen, particularly collagen I and III, the most abundant components of ECM deposition in HS, is considered to be associated with the specific manifestations of HS that is hard and raised above the skin [20]. A previous study by Reanmongkol et al. found that EA has a role in wound healing by a rat dermal wound model, while it is not effective on collagen accumulation [21]. In our study, EA reduced the expression of collagen I and III in HSFs (Fig. 4), similar to a recent study conducted by Lin et al. which demonstrated that EA inhibited the expression of collagen I and III in rat cardiac fibroblasts [9]. This indicates that EA possesses therapeutic potential against fibrosis, which makes it worthy of further research.

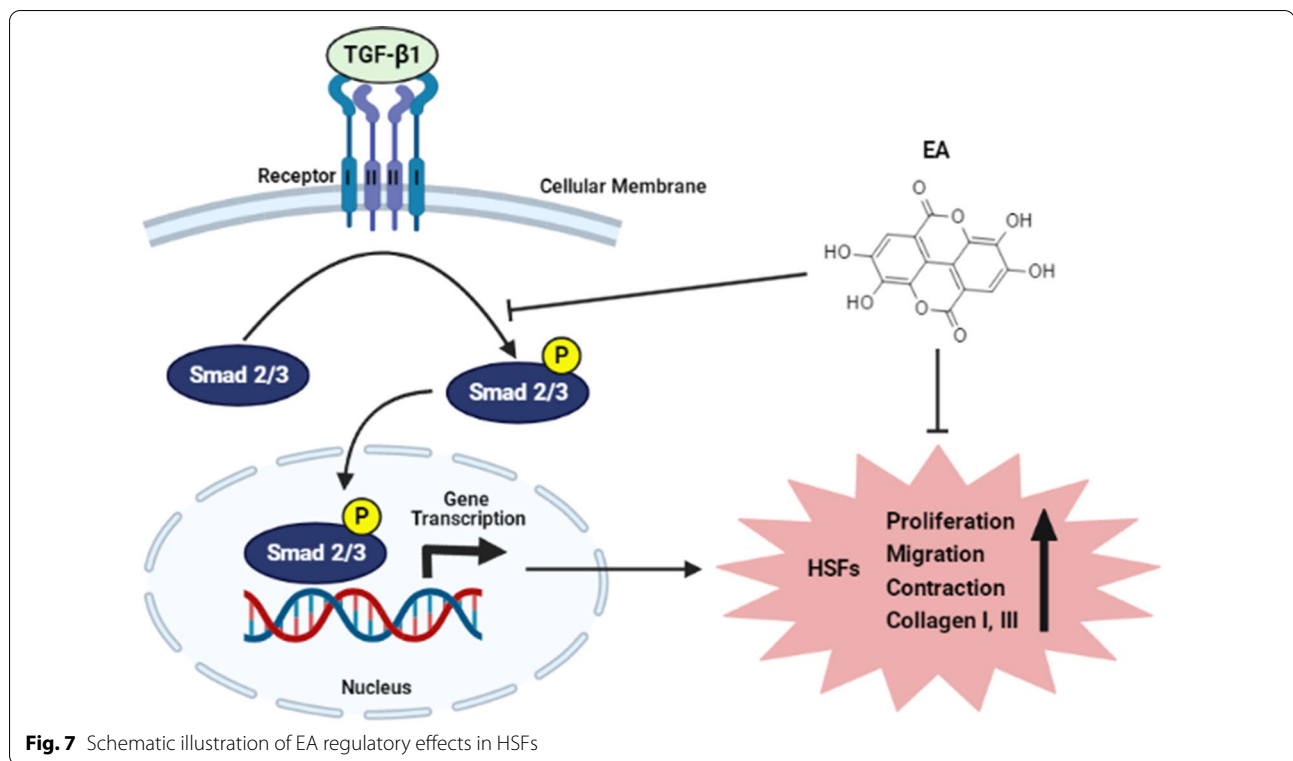
The Smad2/3 pathway is widely recognized as a major signaling pathway that leads to HS formation [3, 22]. Activation of the Smad2/3 pathway causes multiple fibrotic phenotypes of HSFs. TGF- β 1 induces the phosphorylation of Smad2 and 3 by binding to cell surface TGF- β receptors. Phosphorylated Smad2 and 3 translocate to the nucleus with cooperation of Smad4, and these molecules, in the form of a transcriptional complex, regulate downstream target genes expression [23]. Many studies have validated that blocking the TGF- β 1/Smad2/3 pathway can effectively suppress the pathological phenotypes of HSFs [24]. Our study demonstrated that EA suppressed HSFs proliferation, migration, and contraction, and expression of collagen I and III in HSFs by inhibiting the TGF- β 1/Smad2/3 signaling pathway (Fig. 7, created with BioRender.com). However, the upstream mechanism driving EA-induced inhibition of this pathway still



needs further investigation. In addition to mechanism study, further in vivo experiment is needed. A rabbit ear scar model should be a good candidate, which is widely used in the studies on HS [25].

In conclusion, this study demonstrates that EA exerts inhibitory effects on HSFs proliferation, migration, and contraction, and collagen synthesis in HSFs by inhibiting the TGF-β1/Smad2/3 signaling pathway.

These findings present EA as a promising novel drug candidate for treatment of HS, and provide theoretical support for further in vivo experiments and clinical application in the future. Moreover, this research extends our understanding of the biological activity of EA.



Acknowledgements

This study was supported by the PhD Research Project of Jilin Engineering Normal University (no. BSKJ201923), the Fund Project of the Finance Department of Jilin Province (no. JLSWSRCZX2020-002), the Fund Project of the Development and Reform Commission of Jilin Province (no. 2020C049), the Fund Project of Jilin Provincial Science and Technology Department (no. 20200404166YY), and the grants from the First Hospital of Jilin University (no. JDYYGH2019006 and no. BQEGCZX2019004).

We thank Bethune Institute of Epigenetic Medicine of the First Hospital of Jilin University for providing experimental conditions for part of cell experiments in this study.

Authors' contributions

JY and XM designed the concept of the study, reviewed and revised the manuscript. XL and XG wrote the original draft and performed the most experimental tasks. XM, HL, ZL, XW, LZ, BW, and XC performed partial experiments and experimental validation. XM, XL, and XG contributed to results analysis. JY and XL contributed to Funding acquisition. All the authors read and approved the final vision of the manuscript.

Declarations

Competing interest

The authors declare that they have no conflict of interest.

Author details

¹College of Food Engineering, Jilin Engineering Normal University, No. 3050 Kaixuan Street, Changchun 130000, China. ²Measurement Biotechnology Research Center, Jilin Engineering Normal University, No. 3050 Kaixuan Street, Changchun 130000, China. ³Department of Burns Surgery, The First Hospital of Jilin University, No. 1409 Ximinzhu Street, Changchun 130000, China. ⁴Jilin Provincial Skin Repair and Regeneration Engineering Research Center, the First Hospital of Jilin University, No. 1409 Ximinzhu Street, Changchun 130000, China. ⁵Institute for Interdisciplinary Biomass Functional Materials Studies, Jilin

Engineering Normal University, No. 3050 Kaixuan Street, Changchun 130000, China.

Received: 23 June 2021 Accepted: 31 August 2021

Published online: 15 September 2021

References

- Finnerty C, Jeschke M, Branski L, Barret J, Dziewulski P, Herndon D (2016) Hypertrophic scarring: the greatest unmet challenge after burn injury. *Lancet* (London, England) 388(10052):1427–1436
- Bombaro K, Engrav L, Carrougher G, Wiechman S, Faucher L, Costa B et al (2003) What is the prevalence of hypertrophic scarring following burns? *Burns J Int Soc Burn Inj* 29(4):299–302
- Amini-Nik S, Yousuf Y, Jeschke M (2018) Scar management in burn injuries using drug delivery and molecular signaling: current treatments and future directions. *Adv Drug Deliv Rev* 123:135–154
- Ríos J, Giner R, Marín M, Recio M (2018) A pharmacological update of ellagic acid. *Planta Med* 84(15):1068–1093
- García-Niño W, Zazueta C (2015) Ellagic acid: pharmacological activities and molecular mechanisms involved in liver protection. *Pharmacol Res* 97:84–103
- Ceci C, Lacial P, Tentori L, De Martino M, Miano R, Graziani G (2018) Experimental evidence of the antitumor, antimetastatic and antiangiogenic activity of ellagic acid. *Nutrients* 10(11):1756
- Devipriya N, Sudheer A, Srinivasan M, Menon V (2007) Effect of ellagic acid, a plant polyphenol, on fibrotic markers (MMPs and TIMPs) during alcohol-induced hepatotoxicity. *Toxicol Mech Methods* 17(6):349–356
- Suzuki N, Masamune A, Kikuta K, Watanabe T, Satoh K, Shimosegawa T (2009) Ellagic acid inhibits pancreatic fibrosis in male Wistar Bonn/Kobori rats. *Dig Dis Sci* 54(4):802–810
- Lin C, Wei D, Xin D, Pan J, Huang M (2019) Ellagic acid inhibits proliferation and migration of cardiac fibroblasts by down-regulating expression of HDAC1. *J Toxicol Sci* 44(6):425–433

10. Lian N, Li T (2016) Growth factor pathways in hypertrophic scars: Molecular pathogenesis and therapeutic implications. *Biomed Pharmacother Biomed Pharmacother* 84:42–50
11. Livak K, Schmittgen T (2001) Analysis of relative gene expression data using real-time quantitative PCR and the 2(-Delta Delta C(T)) method. *Methods (San Diego, Calif)* 25(4):402–408
12. Zhang J, Li Y, Bai X, Li Y, Shi J, Hu D (2018) Recent advances in hypertrophic scar. *Histol Histopathol* 33(1):27–39
13. Bahri S, Ben Ali R, Abidi A, Jameleddine S (2017) The efficacy of plant extract and bioactive compounds approaches in the treatment of pulmonary fibrosis: A systematic review. *Biomed Pharmacother Biomed Pharmacother* 93:666–673
14. Chen D, Hu H, Wang Y, Feng Y, Cao G, Zhao Y (2018) Natural products for the prevention and treatment of kidney disease. *Phytomed Int J Phytother Phytopharmacol* 50:50–60
15. Domitrović R, Potočnjak I (2016) A comprehensive overview of hepatoprotective natural compounds: mechanism of action and clinical perspectives. *Arch Toxicol* 90(1):39–79
16. Masamune A, Satoh M, Kikuta K, Suzuki N, Satoh K, Shimosegawa T (2005) Ellagic acid blocks activation of pancreatic stellate cells. *Biochem Pharmacol* 70(6):869–878
17. Nedelec B, Ghahary A, Scott P, Tredget E (2000) Control of wound contraction. *Basic Clin Features Hand Clin* 16(2):289–302
18. Namekata I, Hamaguchi S, Wakasugi Y, Ohhara M, Hirota Y, Tanaka H (2013) Ellagic acid and gingerol, activators of the sarco-endoplasmic reticulum Ca²⁺-ATPase, ameliorate diabetes mellitus-induced diastolic dysfunction in isolated murine ventricular myocardia. *Eur J Pharmacol* 706:48–55
19. Olgar Y, Ozturk N, Usta C, Puddu P, Ozdemir S (2014) Ellagic acid reduces L-type Ca²⁺ current and contractility through modulation of NO-GC-cGMP pathways in rat ventricular myocytes. *J Cardiovasc Pharmacol* 64(6):567–573
20. Coentro J, Pugliese E, Hanley G, Raghunath M, Zeugolis D (2019) Current and upcoming therapies to modulate skin scarring and fibrosis. *Adv Drug Deliv Rev* 146:37–59
21. Mo J, Panichayupakaranant P, Kaewnopparat N, Nitiruangjaras A, Reanmongkol W (2014) Wound healing activities of standardized pomegranate rind extract and its major antioxidant ellagic acid in rat dermal wounds. *J Nat Med* 68(2):377–386
22. Shirakami E, Yamakawa S, Hayashida K (2020) Strategies to prevent hypertrophic scar formation: a review of therapeutic interventions based on molecular evidence. *Burns Trauma* 8:tkz003
23. Hu H, Chen D, Wang Y, Feng Y, Cao G, Vaziri N et al (2018) New insights into TGF-β/Smad signaling in tissue fibrosis. *Chem Biol Interact* 292:76–83
24. Zhang T, Wang X, Wang Z, Lou D, Fang Q, Hu Y et al (2020) Current potential therapeutic strategies targeting the TGF-β/Smad signaling pathway to attenuate keloid and hypertrophic scar formation. *Biomed Pharmacother Biomed Pharmacother* 129:110287
25. Domergue S, Jorgensen C, Noël D (2015) Advances in research in animal models of burn-related hypertrophic scarring. *J Burn Care Res* 36(5):e259–e266

Publisher's Note

Springer Nature remains neutral with regard to jurisdictional claims in published maps and institutional affiliations.

Submit your manuscript to a SpringerOpen[®] journal and benefit from:

- Convenient online submission
- Rigorous peer review
- Open access: articles freely available online
- High visibility within the field
- Retaining the copyright to your article

Submit your next manuscript at ► [springeropen.com](https://www.springeropen.com)
